

# On the Structure of Poly(3-hydroxybutanoic acid) in Solution and in Phospholipid Bilayers. Circular Dichroism and Fluorescence Spectroscopy with Oligo(3-hydroxybutanoic acid) Derivatives

Magnus Rueping,<sup>†</sup> Anja Dietrich,<sup>‡</sup> Volker Buschmann,<sup>‡</sup> Monica G. Fritz,<sup>†</sup> Markus Sauer,<sup>‡</sup> and Dieter Seebach<sup>\*†</sup>

Laboratorium für Organische Chemie, Eidgenössische Technische Hochschule, ETH Hönggerberg, CH-8093 Zürich, Switzerland, and Physikalisch-Chemisches Institut, Universität Heidelberg, Im Neuenheimer Feld 253, 69120 Heidelberg, Germany

Received March 26, 2001; Revised Manuscript Received June 12, 2001

**ABSTRACT:** Oligomers of (*R*)-3-hydroxybutanoic acid (OHBs) consisting of 8, 16, and 32 HB units have been investigated by CD spectroscopy in solution and in a racemic phospholipid bilayer. A Freudenberg plot ( $\Theta/n$  vs  $(n-2)/n$ ) of the data obtained in solution can be interpreted as an indication for the presence of a chiral secondary structure of the oligoester chain—on the very short time scale of UV spectroscopy! The OHBs were also combined with fluorescent groups, including donor/acceptor pairs (coumarin, rhodamine, cyanine, oxazine). This enabled their detection by fluorescent microscopy and fluorescence-resonance-energy-transfer (FRET) measurements. With these techniques it was possible to calculate the distance between the fluorescent groups, thus providing information about the conformation of the OHB chain. With a calculated Förster distance  $R_0$  of 60 Å the distance (in  $10^{-6}$  M CHCl<sub>3</sub>) between the termini of HB 8-, 16-, and 32-mer were calculated to be 41, 38, and 49 Å, respectively. This result is compatible with conclusions drawn from other observations, indicating that longer HB chains fold in a hairpin-type fashion. Incorporation of fluorescent 16- and 32-mers in liposomes shows that the latter tend to aggregate while the former do not: The investigation described here did not lead to a decision as to whether an OHB chain, and thus also the poly(hydroxybutanoate) (PHB) chain, attains a  $2_1$ - or a  $3_1$ -helical arrangement in solution.

## Introduction

The polyester poly((*R*)-3-hydroxybutanoate) (PHB), a natural biopolymer, is produced by a variety of microorganisms for use as an intracellular carbon source, as an energy storage material (sPHB), and as storage of reductase equivalents.<sup>1</sup> Low-molecular-weight PHB complexed with CaPP<sub>i</sub> (cPHB) presumably plays an important role in living organisms as it has been detected in eucaryotic and procaryotic cells, in human aorta tissue, and in blood plasma.<sup>2</sup>

Reusch et al. have shown that cPHB and CaPP<sub>i</sub> form a complex that functions as an ion channel in genetically competent *Escherichia coli*.<sup>3</sup> The existence of this non-proteinaceous calcium-selective channel has been proved beyond a doubt in patch-clamp experiments by comparing the complex from *E. coli* membranes with that formed from a synthetic oligo(3-hydroxybutanoic acid) (OHB), containing 128 residues, and inorganic Ca-polyphosphate (ca. 60-mer):<sup>4</sup> an identical, voltage-driven ion transport by a single-channel mechanism was demonstrated for these complexes. OHBs have also been used for preparing complexes with alkaline and alkaline earth salts, and crystal structures have provided ion-channel models.<sup>5</sup> In addition, OHBs alone are able to transport cations across bulk membranes in U-tubes,<sup>6</sup> and they have been shown by patch-clamp experiments to form highly conductive, nonselective, ion channels through lipid bilayers.<sup>7</sup> Finally, and most recently, OHBs of 32, but not 8 or 16, residues, when incorporated in liposomes, were demonstrated to form pores across the bilayer, causing concentration-driven Ca<sup>2+</sup> trans-

port, a kinetic analysis of which indicates that three 32-mers are aggregating to a pore.<sup>8</sup>

The structures of the channels and pores consisting of or containing PHB are unknown. From the required minimum chain length and from the known  $2_1$ -helical structure of PHB chains in lamellar crystallites (thickness ca. 50 Å) and in stretched fibers<sup>9</sup> (Figures 1 and 2) models for the pore and channel structures were derived.<sup>4,8</sup> In those, the  $2_1$ -helices of 6 Å pitch are arranged in columns embedded in the phospholipid bilayer (thickness 40–60 Å), so that ca. 16 residues are required to span the bilayer—and this is the lower-limit chain length with which we have observed ion transport,<sup>7,8</sup> which may or may not be a coincidence. Besides the left-handed  $2_1$ -helix of PHB chains a right-handed  $3_1$ -helix, also of 6 Å pitch, has been identified from single-crystal X-ray structures of cyclic oligomers ("oligolides") (Figure 1).<sup>10</sup> In contrast to these solid-state structures of HB chains, the solution structure is unknown and may be strongly solvent-dependent. Indeed, the conclusions from NMR and optical measurements range from a defined secondary structure<sup>11</sup> all the way to a random-coil structure.<sup>1b</sup>

In this paper, we report on structural investigations of synthetic OHBs with various chain lengths, including OHBs with attached fluorescent dyes, both in solution and in lipid bilayers, using CD spectroscopy as well as fluorescent spectroscopic methods.

## Materials and Methods

**Coupling of OHBs with Dye Molecules.** (*R*)-3-Hydroxybutanoic acid derivatives **1–7** and **15** were synthesized as previously reported<sup>12</sup> (Figure 3). Tetraethylrhodamine was reduced to the corresponding tetraethylrhodamine alcohol and coupled with OHB derivatives in a Yamaguchi esterification

\* To whom correspondence should be addressed.

<sup>†</sup> Laboratorium für Organische Chemie, ETH Zürich.

<sup>‡</sup> Physikalisch-Chemisches Institut, Universität Heidelberg.

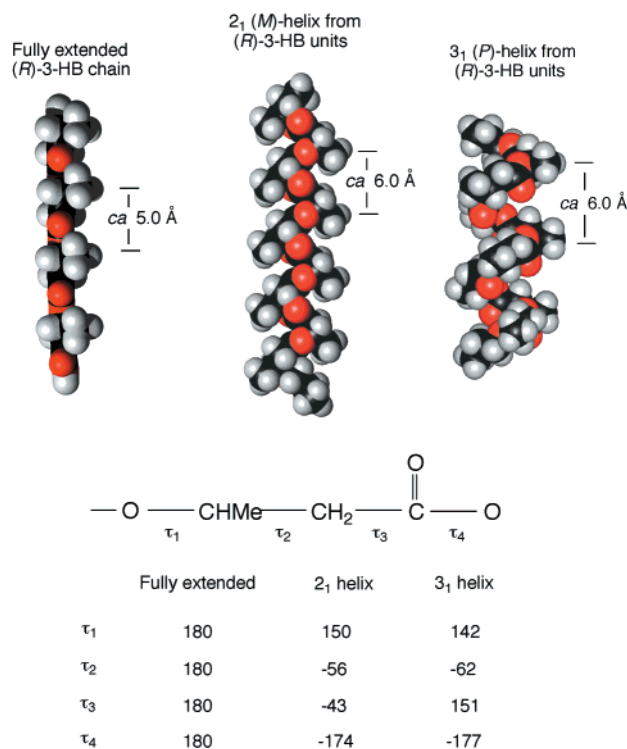
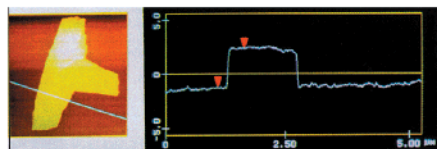


**Figure 1.** HB conformations of a fully extended HB chain and of a 2<sub>1</sub>- and 3<sub>1</sub>-helix. Fully extended HB chain with torsion angles τ<sub>1</sub>–τ<sub>4</sub> set to 180. 2<sub>1</sub>- and 3<sub>1</sub>-helix constructed with the torsions angles of oligolides.<sup>10</sup>

to yield **8**–**10**.<sup>13</sup> Cy5 was obtained as monofunctionalized *N*-hydroxysuccinimidyl ester (Cy5-NHS) from Amersham Life Science Inc. (Cleveland, OH). The oxazine derivative MR121 was kindly provided by Prof. Drexhage (Universität-Gesamthochschule Siegen, Germany). The Cy5-NHS was attached to the Boc-protected amino terminus of tetraethylrhodamine-labeled PHB 8-mer, 16-mer, and 32-mer in carbonate buffer at pH 9.4 and at room temperature (reaction time 3 h) to give the doubly fluorescence-labeled OHBs **11**, **12**, and **14** (Figure 4). The carboxyl group of MR121 was coupled to the amino terminus via in-situ activation, using Castro's reagent,<sup>14</sup> to yield **13**. The reaction was carried out in basic DMF at room temperature for 3 h.

a)



c)

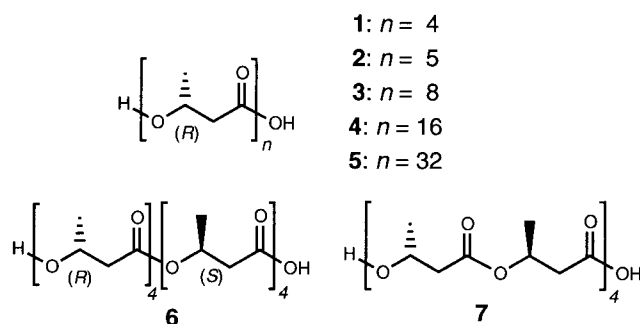
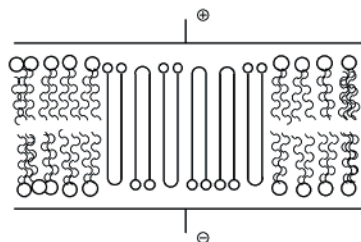


**Figure 3.** Formulas of the synthetic OHB derivatives **1**–**7** used in this investigation.

**HPLC Purification.** The dye-labeled OHBs were purified on an RP18-column, using a gradient of 0–100% acetonitrile in 0.1 M aqueous triethylammonium acetate (TEAA). Retention times: 8-mer-TER **8** (19.5 min), 8-mer-TER/Cy5 **11** (17.9 min), 16-mer-TER **9** (24.5 min), 16-mer-TER/Cy5 **12** (20.8 min), 16-mer-TER/MR121 **13** (22.5 min), 32-mer-TER **10** (49.2 min), and 32-mer-TER/Cy5 **14** (23.4 min).

**Preparation of Liposomes.** Vesicles were prepared as described.<sup>8</sup> POPC was obtained from Avanti Polar Lipids. Racemic POPC were prepared by esterification of oleic acid with *rac*-1-palmitoylglycero-3-phosphocholin, using DCC/DMAP.<sup>15</sup>

**Spectroscopy. Circular Dichroism (CD) Spectra.** All spectra were recorded on a Jasco J-600 from 190 to 400 nm at 20° in a 1 mm rectangular cell with an average of five scans. Corrections for the baseline were accomplished using Jasco software.

**UV and Fluorescence Spectroscopy.** All measurements were carried out at room temperature in nondegassed chloroform (Aldrich) in standard quartz cuvettes with a path length of 1 cm at a concentration of 10<sup>−6</sup> M. Absorption spectra were measured with a Cary 500 UV–vis–NIR spectrophotometer (Varian). Spectra were normalized to the absorption maximum of the donor. Corrected steady-state fluorescence emission and excitation spectra were recorded with a fluorescence spectrophotometer LS100 from Photon Technology Int. (Canada). Fluorescence lifetimes were determined at the emission maxima of the donor and acceptor using a pulsed LED (center wavelength: 495 nm) as an excitation source and time-correlated single-photon counting (TCSPC) with an IBH spectrometer (model 5000MC; Glasgow, Scotland). The instrument response function required for deconvolution was obtained from a

b)



d)

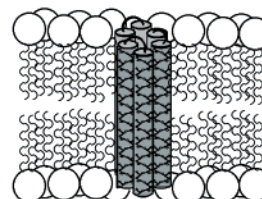


**Figure 2.** Folded structures of the 32-mer **5**. (a) AFM measurements of the thickness of lamellar crystallite of 55 Å.<sup>9e</sup> (b) Lamellar thickness measured with 8-, 16-, and 32-mer (**3**–**5**) and chain structures consisting of 2<sub>1</sub>-helical arrangements (the 2<sub>1</sub>-helix has a pitch of 6 Å).<sup>9d</sup> (c) Proposed model for voltage-driven channels composed of 32-mers.<sup>7</sup> (d) Pore formed from three 32-mers in a vesicle.<sup>8</sup>

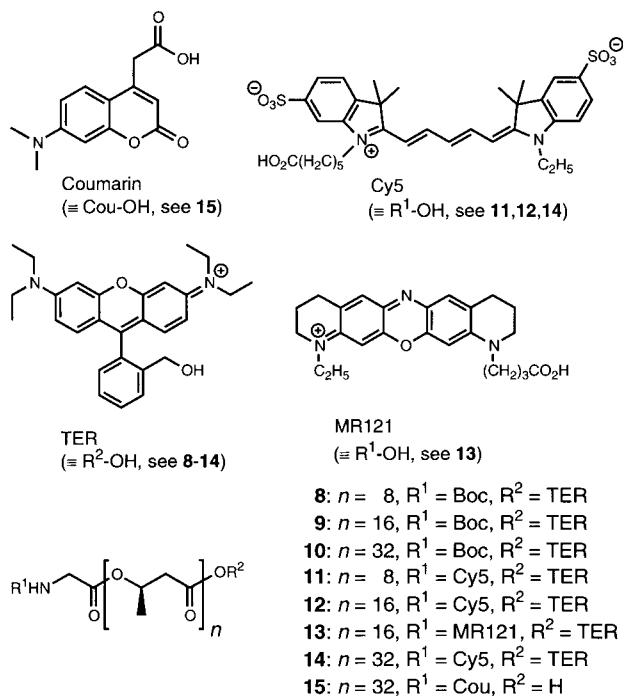


**Figure 4.** Formulas of the fluorescence-labeled HB-oligomers 8–15.

scattering solution. The quality of the decay fits was assessed by means of the reduced chi-squared statistical parameter ( $\chi^2$ ). In most cases, a second component was necessary to fit the decay satisfactorily (eq 1).

$$I(t) = a_1 \exp(-t\tau_1^{-1}) + a_2 \exp(-t\tau_2^{-1}) \quad (1)$$

Here  $a_1$  and  $a_2$  are preexponential factors that describe the ratio of the excited species ( $a_1 + a_2 = 1$ ), and  $\tau_1$  and  $\tau_2$  denote their lifetimes, respectively.

**Scanning Confocal Fluorescence Imaging.** For generation of fluorescence intensity images of liposomes we used a confocal fluorescence microscope equipped with a motion controller-driven  $x, y$ -microscope stage (SCAN 100  $\times$  100, MC2000; Märzhäuser, Wetzlar, Germany). Details about synchronization of scanning and single-photon detection are described in ref 16. For excitation of TER a frequency-doubled Nd:YAG laser with a wavelength of 532 nm (uniphase model 4301-020; München, Germany) was used. The collimated laser beam was directed into an inverted microscope (Axiovert 100TV; Zeiss, Germany) via the backport. Within the microscope the beam was coupled into the microscope objective (100 $\times$ , NA = 1.4; Nikon, Japan) by a dichroic beam splitter (545DRLP; Omega Optics, Brattleboro, VT) and focused onto the liposomes. The average excitation power was adjusted to 5  $\mu$ W at the sample. Fluorescence light emitted by the sample was collected by the objective and focused through the TV outlet of the microscope onto a 50  $\mu$ m pinhole oriented directly in front of an avalanche photodiode (AQR-14; EG&G, Canada). Fluorescence light was spectrally filtered by a band-pass filter (580DF30; Omega Optics, Brattleboro, VT). Fluorescence intensity images were recorded at a resolution of 100 nm/pixel and a collection time of 6 ms/pixel.

## Results and Discussion

**CD Spectroscopy of OHB Derivatives in Solution and in Vesicle Bilayers.** CD spectroscopy is frequently used for the investigation of secondary structures of oligopeptides and proteins in solution. Characteristic CD patterns have also been observed for oligomers of  $\beta$ -amino acids (NH analogues of OHBs).<sup>17</sup> The  $\beta$ -amino acids as well as the  $\beta$ -hydroxy acids contain

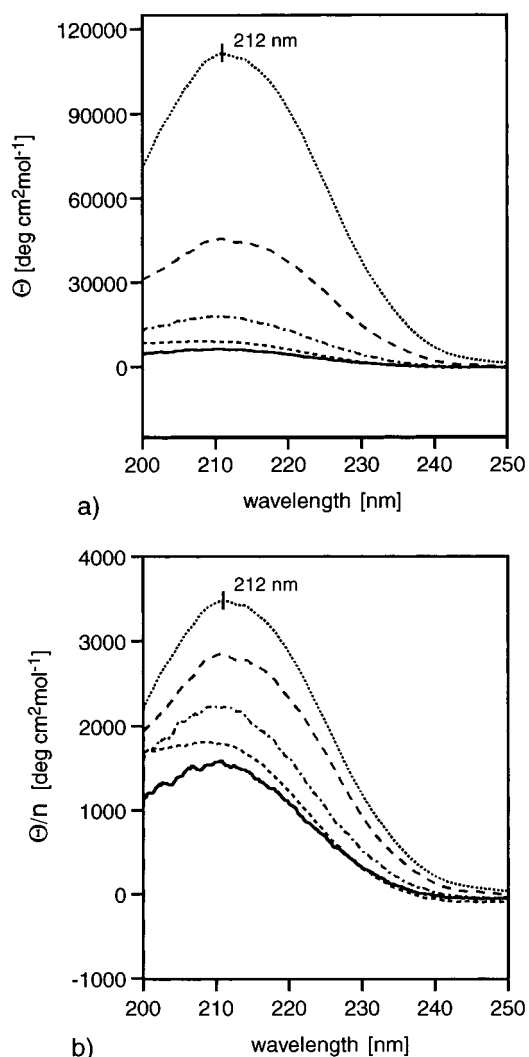


**Figure 5.** CD spectra of HB oligomers 1–5 in trifluoroethanol. (a) Plot of the molar ellipticity  $\Theta$  and (b) plot of the molar ellipticity  $\Theta$  divided by the number of ester bonds per molecule. 1,  $n = 4$  (1 mM) (—); 2,  $n = 5$  (0.8 mM) (---); 3,  $n = 8$  (0.5 mM) (---); 4,  $n = 16$  (0.25 mM) (- - -); 5,  $n = 32$  (0.125 mM) (···).

an ethane unit that favors a staggered arrangement of the chain. Thus, it appeared reasonable to seek an indication for the presence of secondary structures of hydroxybutanoic acid oligomers (OHBs) in solution by CD measurement.

An overlay of the CD spectra of HB oligomers (1–5) in trifluoroethanol is shown in Figure 5a. Indeed, the HB derivatives display a pronounced CD signal with a positive Cotton effect at approximately 210 nm in the region of their UV absorption. To allow for comparison of the spectra, the molarity of the ester carbonyl functionality was kept constant in all the experiments (4 mM, with a resultant molar concentration between 0.12 and 1.00 mM). When the molar ellipticity  $\Theta$  is divided by the number  $n$  of ester bonds per molecule, the spectra shown in Figure 5b result. It is evident that the contribution of each ester bond toward the total ellipticity  $\Theta$  rises significantly with increasing chain length. When the molar ellipticity  $\Theta/n$  is plotted against  $(n - 2)/n$  (following the so-called Freudenberg procedure),<sup>18</sup> a linear relationship results (Figure 6a). This is indicative of an ordered secondary structure and it is not in agreement with a “random coil” structure.

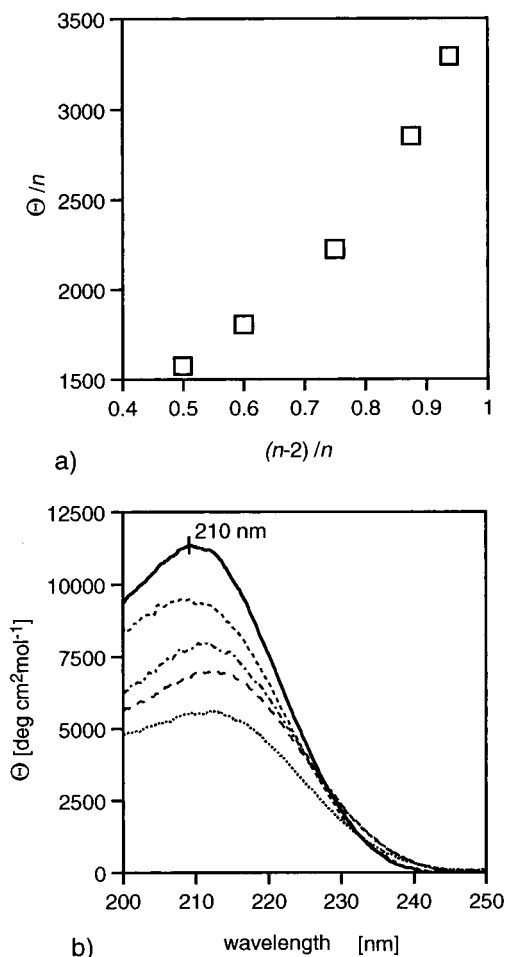


**Figure 6.** Solvent-dependent normalized and nonnormalized CD spectra of OHBs. (a) Plot of the molar ellipticity  $\Theta/n$  vs  $(n-2)/n$  for the HB oligomers **1**–**5** in trifluoroethanol. (b) CD spectra of penta(3-hydroxybutanoic acid) **2** in different solvents (0.8 mM): water (—); trifluoroethanol (---); methanol (····); acetonitrile (- · - ·); octanol (— · —).

The solvent dependence of the CD spectra was examined with the pentamer acid **2** (Figure 6b). The intensity of the positive bands diminishes with decreasing polarity of the solvent ( $\text{H}_2\text{O}$ :  $\Theta = 10\,700 \text{ deg cm}^2 \text{mol}^{-1}$ ; octanol:  $\Theta = 5600 \text{ deg cm}^2 \text{mol}^{-1}$ ). This tendency is compatible with the assumption that hydrophobic interactions (which are weaker in apolar media) contribute to the stability of the structure and is in good agreement with the data reported by Marchessault et al. on PHB.<sup>11a</sup> With diminishing polarity of the medium, a small shift of the maximum ellipticity to higher wavelengths is observed.

We also examined the effect of incorporation (*R*)- and (*S*)-HB units on the CD spectra of OHBs. In Figure 7a of the CD spectra of the *all*-(*R*)-octamer **3** and of the diastereoisomeric compounds **6** and **7** are presented. The incorporation of four (*S*)-HB units in **6** and **7** results in a complete collapse of the characteristic CD patterns, clearly indicating loss of an ordered secondary structure.

By incorporating OHBs in lipid bilayer, the degree of conformational freedom is expected to be restricted, as compared to the situation in solution, and this should influence the pattern of the CD spectra.

Walde et al. have shown that liposomes composed of chiral lipid molecules give characteristic CD-signals in a similar wavelength region as those of the HB derivatives.<sup>19</sup> Thus, OHBs have to be measured in racemic

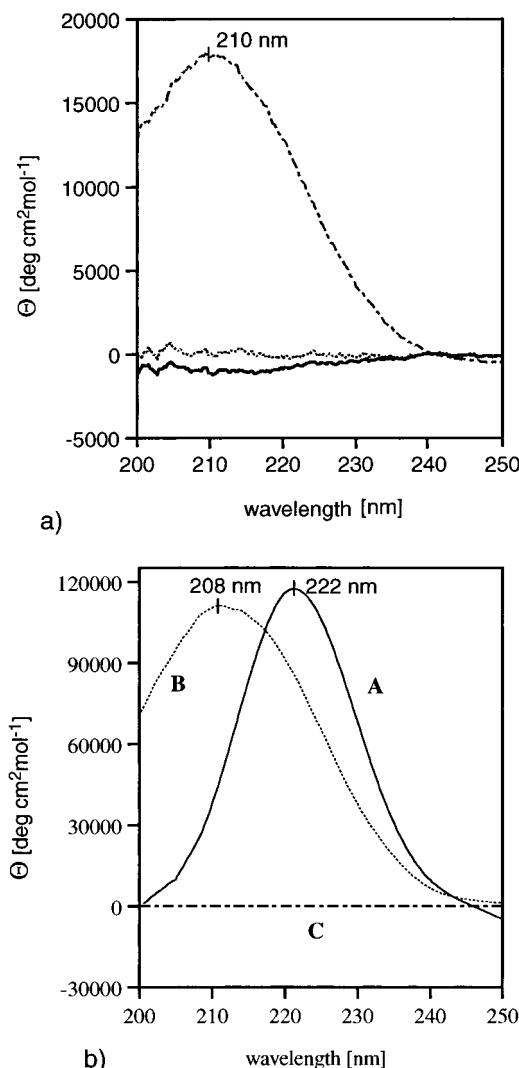


**Figure 7.** CD spectra of various OHB derivatives in trifluoroethanol and in liposomes. (a) Diastereomeric HB octamers in trifluoroethanol (0.5 mM): **3** (---); **6** (····); **7** (—). (b) Fluorescence-labeled dotriacontamer **15**: incorporated in *rac*-POPC (palmitoylcholine) (A, 10.2 mM POPC, 21  $\mu\text{M}$  **15**, in water) and in solution (B, 21  $\mu\text{M}$  **15** in trifluoroethanol). For comparison, the zero line obtained with *rac*-POPC alone is also shown (C, 9.3 mM POPC in water).

POPC. The coumarin-labeled 32-mer **15** was incorporated in liposomes, consisting of *rac*-POPC, as previously described.<sup>8</sup> The maximum molar ellipticity of the OHB derivative in this racemic liposome environment (curve A in Figure 7b) compared to that in  $\text{CF}_3\text{CH}_2\text{OH}$  solution (curve B in Figure 7b) was found to be similar; however, the maximum ellipticity was at longer wavelength in the liposomes (208 nm vs 222 nm). The CD experiments with the pentamer acid **2** (see above) in different solvents indicate that this shift is not a consequence of the apolar environment inside the lipid bilayer. It is conceivable that OHB aggregation in the liposome bilayer (see above) causes the observed effect.

**Fluorescence Measurements in Solution and in Vesicle Bilayers.** To get more detailed information on the conformation in solution, we used fluorescence resonance energy transfer (FRET) to investigate the end-to-end distance of donor/acceptor-labeled OHBs. For this the OHBs were labeled at one end with TER and at the other end with Cy5 and MR121 (see Experimental Section). Distance distributions are of particular interest



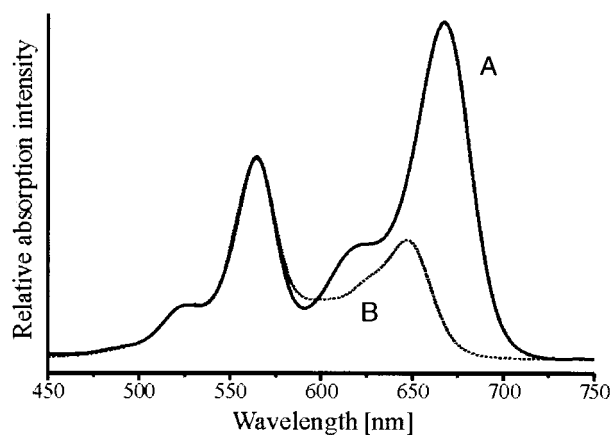


**Figure 8.** Relative absorption spectra of doubly labeled 16-mer OHBs **12** and **13** in  $\text{CHCl}_3$ . (—) TER/Cy5, (···) TER/MR121.

in conformational end-to-end fluctuations of polymers and in protein folding. Since Stryer and Haugland<sup>20</sup> have demonstrated the distance dependence of FRET, this effect has frequently been used as a spectroscopic ruler in experiments with ensembles of molecules,<sup>21–25</sup> and very recently even at the single-molecule level,<sup>25,27</sup> to measure distances in the 10–90 Å range. In FRET, energy is transferred from a donor group to an acceptor group as a result of the coupling between their transition dipoles. The efficiency of the energy transfer,  $E_{\text{FRET}}$ , depends inversely on the sixth power of the distance  $R$  between the donor and the acceptor:  $E_{\text{FRET}} = 1/[1 + (R/R_0)^6]$ , where  $R_0$  is the characteristic or critical distance (Förster distance) at which 50% of the energy is transferred. The distance  $R_0$  is a function of the spectral overlap of donor emission and acceptor absorption  $J(\lambda)$ , of the fluorescence quantum yield of the donor  $\Phi_D$ , of the index of refraction of the medium  $n$ , and the geometrical factor  $\kappa^2$ , which accounts for the relative orientation of the two dipole moments (eq 2).

$$R_0 = [8.79 \times 10^{-5} J(\lambda) \Phi_D \kappa^2 n^{-4}]^{1/6} \quad (2)$$

The transfer efficiency  $E_{\text{FRET}}$  can be determined in different ways: (a) from the decrease of donor fluorescence intensity,<sup>28</sup> (b) from the increase in acceptor fluorescence intensity,<sup>21,29</sup> (c) from the increase in excitation efficiency at the donor absorption maximum monitoring the emission of the acceptor, i.e. from the excitation spectrum,<sup>20</sup> (d) from the depolarization of the donor fluorescence,<sup>24</sup> and (e) from the decrease of the donor fluorescence decay time.<sup>29</sup>

For the OHB derivatives, the Förster distance  $R_0$  at which 50% of the energy is transferred to the acceptor was calculated using the following parameters: the extinction coefficient  $\epsilon$  of the 16-mer labeled with TER **9** in  $\text{CHCl}_3$  at the absorption maximum was measured to be  $\epsilon = 1.2 \times 10^5 \text{ L mol}^{-1} \text{ cm}^{-1}$ , a value which is slightly higher than in ethanol. With this value we calculated extinction coefficients at the absorption maxima in  $\text{CHCl}_3$  of  $\epsilon = 2.0 \times 10^5 \text{ L mol}^{-1} \text{ cm}^{-1}$  for Cy5 (see curve A in Figure 8) and of  $\epsilon = 0.72 \times 10^5 \text{ L mol}^{-1} \text{ cm}^{-1}$  for MR121 (see curve B in Figure 8). The fluorescence quantum yield  $\Phi_f = 0.80$  of the TER-labeled 16-mer **9** in  $\text{CHCl}_3$  was determined using rhodamine 6G as a standard with a fluorescence quantum yield of 0.95 in ethanol, which is nearly temperature-independent.<sup>30</sup> Anisotropy measurements in  $\text{CHCl}_3$  revealed that both the rhodamine and the carbocyanine moiety can rotate

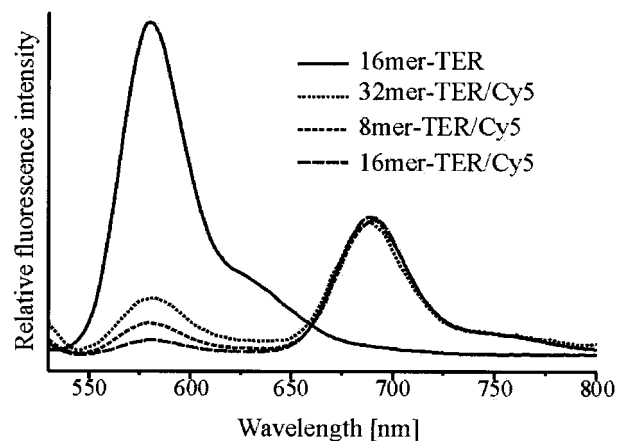


**Figure 9.** Relative emission spectra of TER-labeled 16-mer OHB and TER/Cy5 double-labeled OHBs in  $\text{CHCl}_3$ . Excitation wavelength: 520 nm.

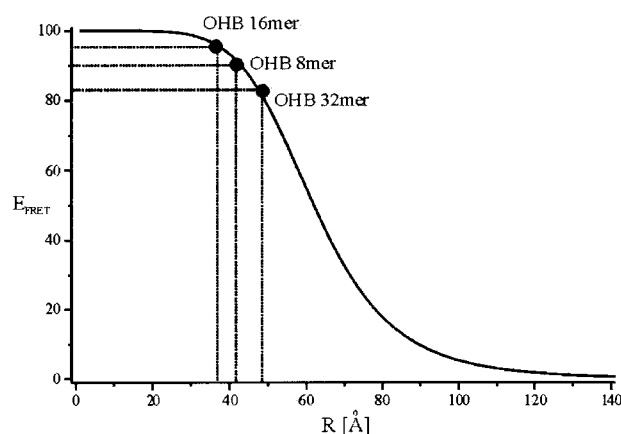


**Figure 10.** Calculated dependence of energy transfer efficiency vs donor–acceptor distance assuming a critical distance of  $R_0 = 62 \text{ Å}$  (Förster distance) for the TER/Cy5 pair on an OHB chain.

**Table 1. Calculated and Measured Distances of OHB Conformations<sup>a</sup>**

OHB	fully extended model	2 <sub>1</sub> -helix <sup>8</sup>	3 <sub>1</sub> -helix model	measured FRET with <b>11</b> , <b>12</b> , <b>14</b>
8-mer	40 Å/93%	24 Å/100%	18 Å/100%	41 Å/90%
16-mer	80 Å/18%	49 Å/80%	36 Å/96%	38 Å/95%
32-mer	160 Å/0%	97 Å/6%	73 Å/27%	49 Å/83%

<sup>a</sup> The % values refer to the  $E_{\text{FRET}}$ , assuming an  $R_0$  of 62 Å for TER/Cy5-labeled OHBs **11**, **12**, and **14**.

freely attached to OHB; i.e.,  $\kappa^2$  can be assumed to be  $2/3$ .

With these values we obtained a critical distance  $R_0$  of 62 Å for the TER/Cy5 donor/acceptor pair covalently attached to OHBs (**11**, **12**, and **14**). From theory, a  $R_0$  value of 62 Å should allow for the determination of donor–acceptor distances between 31 and 92 Å ( $R_0 \pm 50\%$ ). Thus, the donor–acceptor pair used is ideally suited to distinguish between a fully stretched conformation, a 2<sub>1</sub>-helical, and a 3<sub>1</sub>-helical form (see the distances in Table 1). Energy transfer efficiencies of the three OHBs derivatives **11**, **12**, and **14** with 8, 16, and 32 HB residues were calculated from the decrease of donor fluorescence intensity (Figure 9). The calculated energy transfer efficiencies  $E_{\text{FRET}}$  of 83% (32-mer), 90% (8-mer), and 95% (16-mer) are relatively similar (Figure 10, Table 1). Additional data obtained from emission spectra, excitation spectra, and time-resolved fluores-

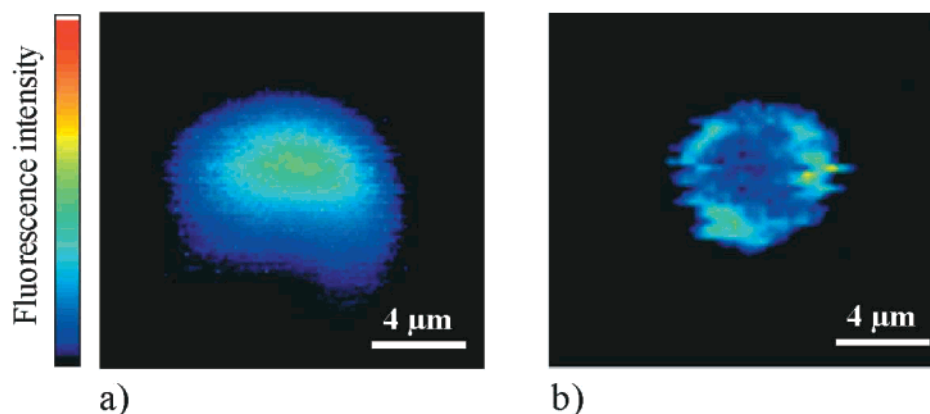


**Figure 11.** Scanning confocal fluorescence intensity images of liposomes including (a) 16-mer **12** and (b) 32-mer OHBs **14**. Average excitation energy at the sample was 5  $\mu$ W.

cence measurements provided the same tendency:  $R_{D/A}$  (32-mer)  $>$   $R_{D/A}$  (8-mer)  $>$   $R_{D/A}$  (16-mer). To support the obtained donor–acceptor distances, Cy5 was exchanged by the oxazine derivative MR121. Although the Förster distance  $R_0$  changed slightly ( $R_0 = 57$  Å as compared to 62 Å) due to the lower extinction coefficient, the TER/MR121-labeled OHB **13** exhibited donor–acceptor distances which were similar to those obtained with the TER/Cy5 pair. From the measured FRET efficiencies the following donor–acceptor distances  $R_{D/A}$  were calculated 41 Å for the 8-mer, 38 Å for the 16-mer, and 49 Å for the 32-mer.

The calculated donor/acceptor distance of 41 Å for the 8-mer OHB **11** implies the existence of an almost fully stretched conformation in  $\text{CHCl}_3$  (see Figure 1, Table 1). In the case of the 16-mer **12** and 32-mer **14** the data are more difficult to interpret in terms of mean distances. In the OHB derivatives the donor and acceptor dye moieties are bound to a relatively flexible polymer chain.<sup>31</sup> Hence, broad distributions of distances may result due to conformational flexibility. While the distance of 38 Å calculated for the OHB 16-mer **12** is compatible with a  $3_1$ -helical structure (see Figure 1, Table 1), the distance of 49 Å obtained for the 32-mer **14** fits neither with a fully extended linear conformation nor with one of the two helical structures as derived from CD spectroscopy in  $\text{CHCl}_3$  (vide supra): it is simply too short! Thus, the ensemble of 32-mer molecules must contain structures in which the ends of the polymer chain are close to each other, for instance in a hairpin arrangement of two chain segments of 16 units with a turn in the middle. For two reasons this is an intriguing result: (a) because the OHB consisting of 32 units had been found to form such hairpins in lamellar crystallites<sup>9d,e</sup> and (b) because this same 32-mer gave perfect single channel events in patch-clamp experiments, as well as concentration-driven  $\text{Ca}^{2+}$  transport through vesicle walls by a pore mechanism. Moreover, the thickness of a phospholipid bilayer is ca. 50 Å, which matches perfectly the length of a 16-mer with  $2_1$ -helical structure (48 Å) or, more importantly, a hairpin structure of a 32-mer with  $2_1$ -helical structure (49 Å). In agreement with these considerations, the proposed model for the ion channel and pore also involves hairpin structures of the 32-mer (see Figure 2).

To further support the proposed ion channel model, liposomes containing labeled 16-mer **12** and 32-mer OHBs **14** have been synthesized and investigated by scanning confocal fluorescence microscopy. As can be seen in Figure 11a, the 16-mer OHBs **12** are more or

less equally distributed in the liposome, which results in a relatively homogeneous fluorescence intensity over the entire liposome. In contrast, the 32-mer OHBs tend to form aggregates clearly recognizable by the bright spots in the membrane (Figure 11b), and this in turn is compatible with the kinetic analysis of the  $\text{Ca}^{2+}$  transport through vesicle walls which indicated that an aggregate of three 32-mers form the ionophoric pore (see above).<sup>8</sup>

## Conclusion

The average distances between termini of the OHBs built of 8, 16, and 32 HB units as calculated from the FRET measurement with the donor/acceptor pair TER/Cy5 (compounds **11**, **12**, and **14**) are compatible with a fully extended 8-mer and secondary structures of the 16-mer and 32-mer which bring the termini closer together than would be possible in a linear arrangement. The interpretation of the FRET measurements support the view that longer HB chains have a tendency to fold, to form turns—not only in the solid state (cf. lamellar crystallites) but also in solution. A clear-cut decision as to whether the HB chains fold in solution to a  $2_1$ - or a  $3_1$ -helix is not possible as conclusion from the FRET measurements.

The CD measurements in three-dimensional-solution and in the two-dimensional phospholipid bilayer environment are also indicative of a chiral secondary structure. The positive Cotton effect near 210 nm of the (*R*)-3-HB-oligomers is in line with an analogous 215 nm maximum exhibited by the oligomers of (*D*)- $\beta$ -amino acids, which are known to form a (*P*) helix (right-handed). In contrast, the  $2_1$ -helix of oligomers of (*R*)-HB is left-handed. Furthermore, the 14 nm bathochromic shift of the Cotton effect of OHBs in a phospholipid bilayer is compatible with the view that the solvent environment is decisive for stabilizing the secondary structure of the oligoester.

The investigations described here support the fact that polyesters, in contrast to polyamides and polypeptides, have highly flexible structures, lacking the stabilizing element of hydrogen bonding.

The fluorescence microscopy of liposomes containing fluorescence-labeled OHB 16-mer and 32-mer is in agreement with the previous finding that 16-mer does not give rise to reproducible  $\text{Ca}^{2+}$  transport through vesicles and that the ion pore generated by OHB 32-mers involves three molecules, i.e., an aggregation of the OHB molecules in the bilayer.

**Acknowledgment.** We thank J. Wolfrum for fruitful cooperation and stimulating discussions and K. H. Drexhage and J. Arden-Jacob for the generous provision of the oxazine derivative M.R.121. Financial support from the Volkswagen-Stiftung (Grant I/74443), ETH (Grant 0-20841-94), and the Bundesministerium für Bildung, Wissenschaft, Forschung und Technologie (Grant 11864 BFA082) is gratefully acknowledged. We express our gratitude to Zeneca Bio Products (Billingham, GB) for supplying us with PHB and Novartis Pharma AG (Basel) for continuing financial support.

## References and Notes

- (1) (a) Schlegel, H. G. *Allgemeine Mikrobiologie*, 7th ed.; Thieme Verlag: Stuttgart, 1992. (b) Doi, Y. *Microbiol Polyesters*; VCH Publishers: Weinheim, Germany, 1990.
- (2) (a) Seebach, D.; Brunner, A.; Bürger, H. M.; Schneider, J.; Reusch, R. N. *Eur. J. Biochem.* **1994**, *224*, 317. (b) Reusch, R. N.; Sparrow, A. W.; Gardiner, J. *Biochim. Biophys. Acta* **1992**, *1123*, 33.
- (3) (a) Reusch, R. N.; Sadoff, H. L. *J. Bacteriol.* **1983**, *156*, 778. (b) Reusch, R. N.; Hiske, T. W.; Sadoff, H. L. *J. Bacteriol.* **1986**, *168*, 553. (c) Reusch, R.; Hiske, T.; Sadoff, H.; Harris, R.; Beveridge, T. *Can. J. Microbiol.* **1987**, *33*, 435. (d) Reusch, R. N.; Sadoff, H. L. *Proc. Natl. Acad. Sci. U.S.A.* **1988**, *85*, 4176. (e) Reusch, R. N. *Proc. Soc. Exp. Biol. Med.* **1989**, *191*, 377. (f) Reusch, R. N. *Chem. Phys. Lipids* **1990**, *54*, 221. (g) Reusch, R. N. *FEMS Microbiol. Rev.* **1992**, *103*, 119. (h) Reusch, R. N.; Huang, R.; Bramble, L. L. *Biophys. J.* **1995**, *69*, 754. (i) Castuma, C. E.; Huang, R.; Kornberg, A.; Reusch, R. N. *J. Biol. Chem.* **1995**, *270*, 12980. (j) Das, S.; Reusch, R. N. *J. Membr. Biol.* **1999**, *170*, 135. (k) Das, S.; Reusch, R. N. *Biophys. J.* **2000**, *78*, 405. (l) Reusch, R. N. *Biochemistry* **2000**, *65*, 280.
- (4) Das, S.; Lengweiler, U. D.; Seebach, D.; Reusch, R. N. *Proc. Natl. Acad. Sci. U.S.A.* **1997**, *94*, 9075.
- (5) Reviews: (a) Müller, H.-M.; Seebach, D. *Angew. Chem., Int. Ed. Engl.* **1993**, *32*, 477. (b) Seebach, D.; Brunner, A.; Bachmann, B. M.; Hoffmann, T.; Kühnle, F. N. M.; Lengweiler, U. D. *Ernst Schering Research Foundation* **1995**, *28*. (c) Seebach, D.; Fritz, M. G. *Int. J. Biol. Macromol.* **1999**, *25*, 217.
- (6) Bürger, H. M.; Seebach, D. *Helv. Chim. Acta* **1993**, *76*, 2570.
- (7) Seebach, D.; Brunner, A.; Bürger, H. M.; Reusch, R. N.; Bramble, L. L. *Helv. Chim. Acta* **1996**, *79*, 507.
- (8) Fritz, M. G.; Walde, P.; Seebach, D. *Macromolecules* **1999**, *32*, 574.
- (9) For PHB see: (a) Yokouchi, M.; Chatani, Y.; Tadokoro, H.; Tani, H.; Teranishi, K. *Polymer* **1973**, *14*, 267. (b) Pazur, J. S.; Raymond, S.; Hocking, P. J.; Marchessault, R. H. *Polymer* **1998**, *39*, 3065. (c) Pazur, J. S.; Raymond, S.; Hocking, P. J.; Marchessault, R. H. *Macromolecules* **1998**, *31*, 6585. For OHB see: (d) Seebach, D.; Bürger, H. M.; Müller, H.-M.; Lengweiler, U. D.; Beck, A. K.; Sykes, K. E.; Parker, P. A.; Barham, P. J. *Helv. Chim. Acta* **1994**, *77*, 1099. (e) Sykes, K. E.; McMaster, T. J.; Miles, M. J.; Parker, P. A.; Barham, P. J.; Seebach, D.; Müller, H.-M.; Lengweiler, U. D. *J. Mater. Sci.* **1995**, *30*, 623.
- (10) (a) Plattner, D. A.; Brunner, A.; Dobler, M.; Müller, H.-M.; Petter, W.; Zbinden, P.; Seebach, D. *Helv. Chim. Acta* **1993**, *76*, 2581. (b) Seebach, D.; Hoffmann, T.; Kühnle, F. N. M.; Lengweiler, U. D. *Helv. Chim. Acta* **1994**, *77*, 2007.
- (11) (a) Marchessault, R. H.; Okamura, K.; Su, C. J. *Macromolecules* **1970**, *3*, 735. (b) Cornibert, J.; Marchessault, R. H.; Benoit, H.; Weill, G. *Macromolecules* **1970**, *3*, 741. (c) Kamiya, N.; Inoue, Y.; Yamamoto, Y.; Chujo, R.; Doi, Y. *Macromolecules* **1990**, *23*, 1313. (d) Li, J.; Uzawa, J.; Doi, Y. *Bull. Chem. Soc. Jpn.* **1998**, *71*, 1683. (e) Seebach, D.; Rueping, M.; Waser, P.; Duchardt, E.; Schwalbe, H. *Helv. Chim. Acta* **2001**, *84*, 1821. (f) Marchessault, R. H.; Yu, G. In *Handbook of Biopolymers*; Steinbüchel, A., Doi, Y., Eds.; Wiley/VCH: New York, 2001; Vol. 5.
- (12) (a) Lengweiler, U. D.; Fritz, M. G.; Seebach, D. *Helv. Chim. Acta* **1996**, *79*, 670. (b) Fritz, M. G.; Seebach, D. *Helv. Chim. Acta* **1998**, *81*, 2414.
- (13) Inanaga, J.; Hirata, K.; Saeki, H.; Katsaki, T.; Yamaguchi, M. *Bull. Chem. Soc. Jpn.* **1979**, *52*, 1989.
- (14) Castro, B.; Dormoy, J. R.; Evin, G.; Selve, C. *Tetrahedron Lett.* **1975**, *14*, 1219.
- (15) Höfle, G.; Steglich, W.; Vorbrüggen, H. *Angew. Chem., Int. Ed. Engl.* **1978**, *17*, 569.
- (16) Tinnefeld, P.; Buschmann, V.; Herten, D.-P.; Han, K.-T.; Sauer, M. *Single Mol.* **2000**, *1* (3), 215.
- (17) (a) Nakanishi, E. K.; Berova, N.; Woody, R. W. *Circular Dichroism*; VCH: New York, 1994. (b) Seebach, D.; Ciceri, P. E.; Overhand, M.; Jaun, B.; Rigo, D.; Oberer, L.; Hommel, U.; Amstutz, R.; Widmer, H. *Helv. Chim. Acta* **1996**, *79*, 2043.
- (18) Freudenberg, K.; Blomquist, C. *Chem. Ber.* **1935**, *68*, 2070.
- (19) Walde, P.; Blöchliger, E. *Langmuir* **1997**, *13*, 1668.
- (20) Stryer, L.; Haugland, R. P. *Proc. Natl. Acad. Sci. U.S.A.* **1967**, *58*, 719.
- (21) Clegg, R. M. *Methods Enzymol.* **1992**, *211*, 353.
- (22) Selvin, P. R. *Methods Enzymol.* **1995**, *246*, 300.
- (23) Gohlke, C.; Murchie, A. I. H.; Lilley, D. M. J.; Clegg, R. M. *Proc. Natl. Acad. Sci. U.S.A.* **1994**, *91*, 11660.
- (24) Parkhurst, K. M.; Parkhurst, L. J. *Biochemistry* **1995**, *34*, 293.
- (25) Norman, D. G.; Grainger, R. J.; Uhrin, D.; Lilley, D. M. J. *Biochemistry* **2000**, *39*, 6317.
- (26) Ha, T.; Enderle, Th.; Ogletree, D. F.; Chemla, D. S.; Selvin, P. R.; Weiss, S. *Proc. Natl. Acad. Sci. U.S.A.* **1996**, *93*, 6264.
- (27) Deniz, A. A.; Dahan, M.; Grunwell, J. R.; Ha, T.; Faulhaber, A. E.; Chemla, D. S.; Weiss, S.; Schultz, P. G. *Proc. Natl. Acad. Sci. U.S.A.* **1999**, *96*, 3670.
- (28) Epe, B.; Steinhäuser, K. G.; Woolley, P. *Proc. Natl. Acad. Sci. U.S.A.* **1983**, *80*, 2579.
- (29) Dale, R. E.; Eisinger, J. In *Biochemical Fluorescence: Concepts*; Chen, R. F., Edelhoof, H., Eds.; Marcel Dekker: New York, 1975; Vol. 1, pp 238–239.
- (30) Hochstrasser, R. M.; Chen, S. M.; Millar, D. P. *Biophys. Chem.* **1992**, *45*, 133.
- (31) Yang, M.; Millar, D. P. *Biochemistry* **1996**, *35*, 7959.
- (32) Arden-Jacob, J. Dissertation, Universität-Gesamthochschule Siegen, 1992.
- (33) Huglin, M. B.; Radwan, M. A. *Polymer* **1991**, *32*, 1293.

MA010520U